Growth Cone Collapse through Coincident Loss of Actin Bundles and Leading Edge Actin without Actin Depolymerization

Feng-quan Zhou and Christopher S. Cohan

Department of Anatomy and Cell Biology, State University of New York at Buffalo, Buffalo, New York 14214

Abstract. Repulsive guidance cues can either collapse the whole growth cone to arrest neurite outgrowth or cause asymmetric collapse leading to growth cone turning. How signals from repulsive cues are translated by growth cones into this morphological change through rearranging the cytoskeleton is unclear. We examined three factors that are able to induce the collapse of extending *Helisoma* growth cones in conditioned medium, including serotonin, myosin light chain kinase inhibitor, and phorbol ester. To study the cytoskeletal events contributing to collapse, we cultured *Helisoma* growth cones on polylysine in which lamellipodial collapse was prevented by substrate adhesion. We found that all three factors that induced collapse of extending growth cones also caused actin bundle loss in polylysine-attached growth cones without loss of actin meshwork. In addition, actin bundle loss correlated with specific filamentous actin redistribution away from the leading edge that is characteristic of repulsive factors. Finally, we provide direct evidence using time-lapse studies of extending growth cones that actin bundle loss paralleled collapse. Taken together, these results suggest that actin bundles could be a common cytoskeletal target of various collapsing factors, which may use different signaling pathways that converge to induce growth cone collapse.

Key words: growth cone • collapse • actin filaments • actin bundles • axon guidance

Introduction

Growth cones at the growing tips of axons play a critical role in controlling axon elongation and pathfinding during the development of the nervous system. The extracellular guidance cues, either attractive or repulsive, bind their specific receptors on growth cones and then transduce the signals through different pathways and eventually induce directed axon growth (Tessier-Lavigne and Goodman, 1996). So far, many guidance molecules and their receptors have been identified (Mueller, 1999). However, it remains unclear how the growth cone integrates the signals from different cues that it encounters at any one time and then translates them into the asymmetrical cytoskeletal rearrangement associated with steering.

It is possible that both attractive and repulsive guidance cues induce growth cone steering through a small number of common cytoskeletal events. For instance, it has been shown that when growth cones contact different attractive cues, either a target cell or NGF beads, F-actin rapidly becomes concentrated at the site where the growth cone will turn, followed by lamellipodia protrusion in that direction (Lin and Forscher, 1993; Gallo and Letourneau, 2000). Thus, it is believed that local accumulation of F-actin and the following lamellipodia protrusion represent a set of common cytoskeletal events when growth cones respond to attractive cues (Bentley and O'Connor, 1994).

It has been shown that repulsive cues can cause the collapse of the whole growth cone, a process involving retraction of the filopodia and lamellipodia (Fan et al., 1993). This phenomenon has been widely used to study repulsive axon guidance molecules in vitro (Cox et al., 1990; Luo et al., 1993), and it is widely accepted that localized growth cone collapse is the mechanism underlying repulsive axon steering (Fan and Raper, 1995). Therefore, elucidating the cytoskeletal mechanism of growth cone collapse will not only allow us to understand how repulsive guidance signals are interpreted by growth cone cytoskeleton but also help us identify potential candidates that link guidance cues to the cytoskeleton. However, in contrast to cytoskeletal rearrangement when growth cones contact attractive cues there is little information about cytoskeletal changes associated with growth cone collapse. Raper and colleagues have described the semaphorin 3A (collapsin)–induced growth cone collapse from which they concluded that the collapse of the growth cone is attributable to reduction of F-actin concentration, especially from the leading edge of the growth cone (Fan et al., 1993). Unfortunately, further study to reveal the cytoskeletal events beyond this is prevented by collapse itself.

Address correspondence to Christopher S. Cohan, Dept. of Anatomy and Cell Biology, State University of New York at Buffalo, Buffalo, NY 14214. Tel.: (716) 829-3081. Fax: (716) 829-2915. E-mail: ccohan@buffalo.edu

In this study, we use *Helisoma* growth cones cultured on polylysine substrate in defined medium (DM)[1] in which lamellipodial collapse was prevented by substrate adhesion to study the cytoskeletal events contributing to growth cone collapse. Under this condition, we examined three growth cone collapsing factors, including neurotransmitter serotonin, myosin light chain kinase (MLCK) inhibitor, and soluble ligand phorbol-ester (phorbol-12 myristate 13-acetate [TPA]), which all have been shown to induce growth cone collapse (Haydon et al., 1984; Ruchhoeft and Harris, 1997; Fournier et al., 2000), to see how they affect growth cone cytoskeleton. First, we found that they all induce actin bundle loss in polylysine-attached (PA) growth cones, and this is correlated with collapse of extending growth cones. Second, we demonstrated that actin bundle loss induced decreased actin assembly at the leading edge that results from coordinated actin filament reorganization rather than direct inhibition of actin polymerization. Third, three different collapsing factors induced similar actin bundle loss through different signal transduction pathways. Finally, we showed directly, using time-lapse studies of extending growth cones, that actin bundle loss paralleled collapse. Taken together, these results suggest that F-actin reorganization through actin bundles could be the cytoskeletal mechanism underlying growth cone collapse, and actin bundles may be common cytoskeletal targets of various collapsing factors, which may use different signaling pathways that converge to induce growth cone collapse.

Materials and Methods

Materials

1-(5-iodonaphthalene-1-sulfonyl)-1H-hexahydro-1,4-diazepine-HCl (ML-7), KT-5720, and wortmannin (WT) were purchased from Calbiochem-Novabiochem; 1-(5-isoquinolinesulfnyl)-2-methylpiperazine, 2HCl (H-7), staurosporine (STS), bisindolylmaleimide I (BIS), 2,3-butanedione monoxime (BDM), serotonin, TPA, cytochalasin D, phalloidin, L-polylysine, and lanthanum were from Sigma-Aldrich; bodipy FL phallacidin was from Molecular Probes; lysophosphatidic acid (LPA) was from Cayman Chemical; and salt-free liebowitz L-15 medium was made by GIBCO BRL.

Cell Culturing

For experiments conducted on PA growth cones, neurons with attached axons were removed from the buccal ganglia *of Helisoma trivolvis* as described by Williams and Cohan (1994) and plated onto polylysine-coated coverslips. Cells were cultured in DM L-15 supplemented with 40 mM NaCl, 1.7 mM KCl, 4.1 mM $CaCl_2$, 1.5 mM $MgCl_2$, 1 mM glutamine, and 10 mM Hepes, pH 7.4, at room temperature. In the experiments, we chose growth cones that were at the stage of 1–1.5 h after plating. For experiments involving serotonin, only growth cones from identified neuron B19 were used.

For growth cone collapse experiments, neurons were cultured in the medium containing conditioning factors prepared from *Helisoma* brain ganglia (Wong et al., 1981). Brains were transferred into a 35-mm plastic Petri dish with 2 ml DM and incubated for 72 h. Neurons were then cultured in the conditioned medium (CM) for 8–16 h to allow neurite outgrowth.

[1]*Abbreviations used in this paper:* BDM, 2,3-butanedione monoxime; BIS, bisindolylmaleimide I; C-domain, central domain; CM, conditioned medium; DM, defined medium; ERM, ezrin/radixin/moesin; LPA, lysophosphatidic acid; MLCK, myosin light chain kinase; ML-7, 1-(5-Iodonaphthalene-1-sulfonyl)-1H-hexahydro-1,4-diazepine-HCl; PA, polylysine attached; P-domain, peripheral domain; STS, staurosporine; TPA, phorbol-12 myristate 13-acetate; WT, wortmannin.

Drug Application

All chemical agents used in the experiments were cell permeable and were diluted from the stock solution to the final concentration with the medium. They were then perfused into the culture chamber during the experiments. Since LPA precipitates in the medium containing calcium, it was diluted using the medium containing 0.5–1% fatty acid–free BSA, which has been reported to enhance the solubility of LPA (Jalink et al., 1990). All experiments related to LPA were also done in the medium containing BSA.

Videomicroscopy

Growth cones were viewed with an inverted light microscope (Nikon) equipped with a dry condenser (0.52 NA) for phase–contrast optics. Images of the growth cones were recorded with a cooled CCD camera (Photometrics Ltd.) controlled by IPLab Spectrum software (Signal Analytics) after 2.5× projection. For PA growth cones, a 40× oil immersion phase objective (1.30 NA) was used and images were acquired immediately before treatments and at 15, 30, 45, and 60 min after treatments. For extending CM growth cones, a 20 or 40× phase objective (0.75 NA) was used. All image processing, including contrast enhancement and pseudocolor rendering, was done with IPLab Spectrum.

Fluorescence Microscopy

For fluorescent staining, cells were fixed in glutaraldehyde, lysed, and stained with bodipy FL phallacidin for actin as described in Welnhofer et al. (1997). After growth cones were labeled, they were viewed with the fluorescent microscope system (300 Diaphot; Nikon), consisting of 100×, 1.25 NA oil objective lens and a 2× projector lens. Digital images were then acquired with a CCD camera (Princeton Instruments) controlled by IPLab software.

Growth Cone Collapse Assay

Growth cones cultured in the CM were observed and images were acquired before and after 30 min under each of the following conditions: (a) for control, no drug was added to the medium; (b) 5 μM ML-7; (c) 10–20 μM LPA for 15–20 min, followed by 5 μM ML-7; (d) 100 nM TPA; (e) 0.2 μM BIS for 15–20 min, followed by 100 nM TPA. The total number of growth cones in all cells after each treatment was counted. Only growth cones with both filopodia and lamellipodia were counted. The percentage of collapsed growth cones was calculated as the percentage of decrease of the number of growth cones after each treatment.

Growth Cone Formation Assay

Axons of neurons were cut and the PA growth cone formation process was observed for 1 h under the following conditions: (a) control; (b) 50 μM ML-7; (c) 10–20 μM LPA for 15–20 min, followed by 50 μM ML-7. The number of cut axons that formed growth cone within 1 h of axotomy under each condition was counted.

Measurement and Data Analysis

All measurements were made with IPLab Spectrum image analysis software. To measure the number of actin bundles per unit length, we drew lines with fixed length (100 pixels) that were perpendicular to the actin bundles and close to the leading edge of the growth cone. The number of the lines drawn in each growth cone depended on the size of the growth cone. In each case, the whole fan-shaped lamellipodial area was analyzed. We then counted the number of actin bundles that crossed each line and averaged them in each growth cone to obtain the final measurement represented as the number of bundles per 100-pixel length. The change in actin bundle number per unit length with time (1 h) in the experiments was expressed by converting the numbers to a percentage value compared with the initial number at time zero.

To measure filopodia lengthening, time-lapse movies were made with 20 frames (interval of 15 s). The movie was started right after filopodia began to lengthen (usually within 5 min after drug treatment). To measure filopodia elongation rate, only filopodia that elongated continuously for at least four frames were picked. The displacement of the filopodia tips was then measured (in four frames), and the rate was calculated with the unit of μm/min. To measure filopodial length change, filopodia length was measured at time zero and 10 min after drug treatment. 20 filopodia were randomly chosen from each growth cone. Filopodial lengths were determined by

measuring from the edge of the lamellipodia to the distal end of the filopodia. Filopodial length change was represented as the average percentage value of filopodial length after 10 min of treatment versus time zero.

The fluorescent intensity profile of actin filament meshwork was obtained from the intensity versus distance profile of a line (3 pixels wide) drawn parallel to the actin bundles of phallacidin-stained growth cones. The lines were drawn across the actin meshwork between actin bundles in control growth cones. The actin clumps near the central domain were avoided. Each line was divided equally into five parts, and intensity values within each part were averaged and then normalized to the highest intensity part. Five lines were selected randomly from each growth cone, and their respective percentage intensity values were averaged to produce the final distance versus relative intensity plots.

Statistics

All data were reported as mean ± SEM, and we used unpaired Student's *t* test to determine the significance of the data. For percentage data, the χ^2 test was used.

Results

Serotonin Induces Actin Bundle Loss in Helisoma Growth Cones

Neurotransmitters are widely accepted as a group of physiological diffusible axon guidance cues (Tessier-Lavigne, 1994; Zheng et al., 1994, 1996). Serotonin is the first soluble agent that has been shown to play an important role in regulating growth cone motility and neurite extension (Haydon et al., 1984; Kater and Mills, 1991). It has been shown to specifically stimulate the collapse of identified *Helisoma* neuron B19 growth cones cultured in CM and therefore arrests neurite growth both in vitro and in vivo (Budnik et al., 1989; Goldberg and Kater, 1989). In addition, serotonin can also induce the collapse of chick dorsal root ganglion neuron growth cones (Igarashi et al., 1995). To study the cytoskeletal mechanism of serotonin-induced growth cone collapse, we cultured *Helisoma* B19 neurons on polylysine-coated coverslips. Under this condition, instead of forming motile growth cones larger and nonmotile growth cones form at the tip of the axon. These large growth cones do not collapse due to high adhesion of their membrane to the polylysine-coated substrate. Fig. 1 A shows a PA growth cone with characteristic morphology, which shares similar cytoskeletal features with extending CM growth cones (Williams and Cohan, 1994). The phase-dense linear structures are actin bundles that span the whole peripheral area (P-domain) of the growth cone (Welnhofer et al., 1997). The distal ends of the actin bundles protrude from the lamellipodia to form the filopodia. When these growth cones (from B19 neurons) were treated with serotonin, we found that there was a dramatic actin bundle loss (Fig. 1 B). Quantitative analysis showed that after a 1-h treatment, actin bundle density dropped significantly compared with the control (38.73 vs. 82.19% in control; see Fig. 4 B). Another neurotransmitter, dopamine, which also causes growth cone collapse of B19 (McCobb et al., 1988) and vertebrate neurons (Lankford et al., 1988) and acts as a target-derived guidance cue (Spencer et al., 2000), induced similar actin bundle loss in PA B19 growth cones (data not shown). Because both neurotransmitters cause collapse of the same neuron cultured in CM, this result shows a correlation between CM growth cone collapse and actin bundle loss of PA growth cones, suggesting that actin bundle loss might be an underlying mechanism of the collapse.

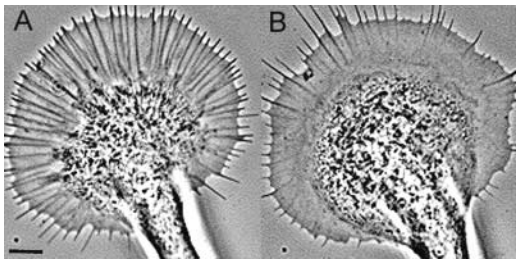

Figure 1. Serotonin induces actin bundle loss from growth cones. *Helisoma* B19 growth cones cultured on polylysine were treated with 100 μM serotonin for 1 h and visualized by phase–contrast microscopy. Before treatment, there were abundant actin bundles (phase-dense linear structures) across the growth cone peripheral area (A). After serotonin treatment, there was dramatic actin bundle loss (B). Bar, 5 μm.

Two Other Collapsing Factors, ML-7 and TPA, Induce Similar Effects as Serotonin

To further confirm the correlation between actin bundle loss in PA growth cones and CM growth cone collapse, we tested two other factors that both are able to induce growth cone collapse. ML-7 is a compound that is structurally unrelated to ATP but can bind specifically at or near the ATP-binding site of MLCK. Therefore, it inhibits the transfer of phosphate from MLCK to its substrate, myosin light chain, which is required for myosin II activation. It has been shown to induce collapse of *Xenopus* retinal ganglia cell growth cones both in vivo and in vitro (Jian et al., 1994; Chien and Harris, 1996; Ruchhoeft and Harris, 1997). First, we tested if ML-7 also induced collapse of *Helisoma* CM growth cones. Application of ML-7 resulted in total growth cone collapse with loss of both lamellipodia and filopodia that produced a club-like morphology (Fig. 2, A compared with B). Retraction of neurites was also observed during ML-7 application (Fig. 2 B). The collapse was dose dependent (data not shown), and 5 μM ML-7 induced a significant percentage of growth cone collapse (74%) within 30 min compared with the control (6%). After washing out the ML-7, most growth cones recovered within 30 min with reformation of new filopodia and lamellipodia (Fig. 2 C).

To examine the effects of ML-7 on PA growth cone morphology, 10 μM ML-7 was added to the medium. Within 1 h after drug application, ML-7 also caused a dramatic loss of actin bundles in the growth cone (Fig. 2, D compared with E). The effect of ML-7 occurred in a concentration- and time-dependent manner and was also reversible (Fig. 2, F–H). In addition, we also tested TPA, an activator of PKC, which has been shown to induce chick dorsal root ganglion growth cone collapse similar to that of semaphorin 3A and myelin (Fournier et al., 2000). When TPA was applied to *Helisoma* CM growth cones, it also induced significant growth cone collapse (77%; Fig. 3, A compared with B). Similarly, TPA induced actin bundle loss in PA growth cones through fascin inactivation as shown previously (Cohan et al., 2001). Taken together, our results strongly correlate CM growth cone collapse with actin bundle loss of PA growth cones.

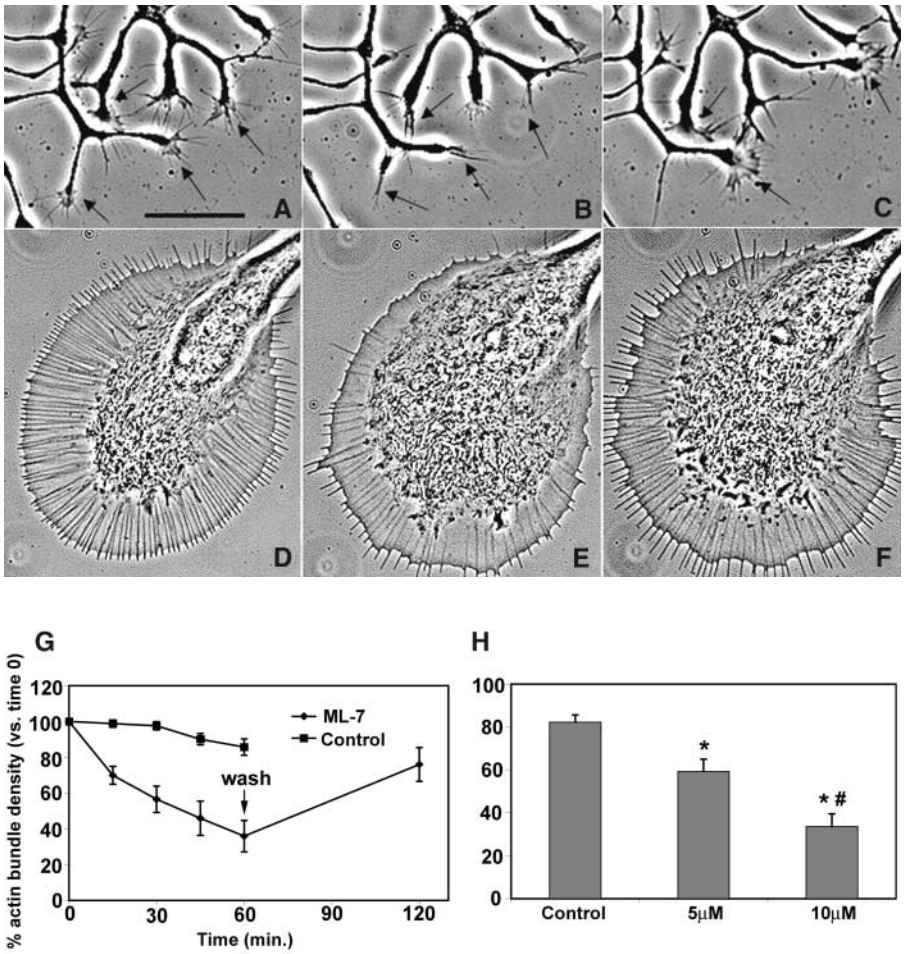

Figure 2. MLCK inhibitor ML-7–induced growth cone collapse in CM correlates with actin bundle loss in PA growth cones. When ML-7 was added onto growth cones cultured in CM, it induced significant growth cone collapse (B) and neurite retraction (arrows) compared with before application (A). When PA growth cones (D) were treated with ML-7, actin bundle loss occurred (E). Both effects were reversible. Growth cones in CM and actin bundles in PA growth cones reformed after washing out the ML-7 (C and E). ML-7–induced actin bundle loss was dose and time dependent (G and H). $*P < 0.0005$, significant difference from control; $\#P < 0.005$, significant difference from 5 μM ML-7. Bar: (A–C) 40 μm; (D–F) 20 μm.

Treatments That Antagonize Growth Cone Collapse in CM also Block Actin Bundle Loss in PA Growth Cones

We also examined whether treatments that inhibited collapse inhibited actin bundle loss. It has already been shown that calcium influx is responsible for serotonin-induced *Helisoma* growth cone collapse (Cohan et al., 1987; Kater and Mills, 1991; Polak et al., 1991). Therefore, we tested whether a block of calcium influx also prevented actin bundle loss caused by serotonin in PA growth cones. We used general calcium channel blocker lanthanum, which has been shown to block calcium influx in *Helisoma* growth cones (Welnhofer et al., 1999). Our results showed that lanthanum significantly antagonized the effect of serotonin on actin bundles (Fig. 4 B).

ML-7–induced growth cone collapse and actin bundle loss are likely through inhibition of MLCK and subsequent myosin II inactivation. Myosin II is activated by MLCK-mediated myosin light chain phosphorylation and deactivated by myosin light chain phosphatase (Bresnick, 1999). LPA has been shown to activate Rho kinase, a small GTPase RhoA-dependent kinase (Kimura et al., 1996; Moolenaar et al., 1997), which can either directly phosphorylate myosin light chain at the same site as MLCK (Amano et al., 1996) or inhibit myosin light chain phosphatase (Kimura et al., 1996). Therefore, LPA treatment results in increased phosphorylation of myosin light chain and keeps it active even when MLCK is inhibited. To determine whether LPA could rescue the ML-7–induced growth cone collapse, we pretreated cells in CM with LPA for 15–30 min and then applied the ML-7 in the presence of LPA. Our results show that pretreatment of growth cones with LPA significantly prevented growth cone collapse induced by ML-7 (Fig. 4 A). To determine whether LPA could also prevent the loss of actin bundles caused by MLCK inhibition, we pretreated PA growth cones with LPA for 15–30 min and then applied ML-7 in the presence of LPA. Similarly, we found that the effects of ML-7 on actin bundles were totally abolished (Fig. 4 B), indicating that LPA antagonizes the effect of MLCK inhibition on both CM and PA growth cones.

Because TPA is a specific PKC activator, it is very likely that its effects on growth cones are through PKC activation. Indeed, when cells were pretreated with the specific PKC inhibitor BIS, both TPA-induced CM growth cone collapse and actin bundle loss in PA growth cones were significantly blocked (Fig. 4, A and B). Together, these results further support the correlation between actin bundle loss and growth cone collapse.

Effects of Collapsing Factors on Actin Reorganization in PA Growth Cones

We tested how actin bundle loss influenced F-actin organization in PA growth cones. Fig. 5 A shows a PA growth cone stained with fluorescent-labeled phalloidin under

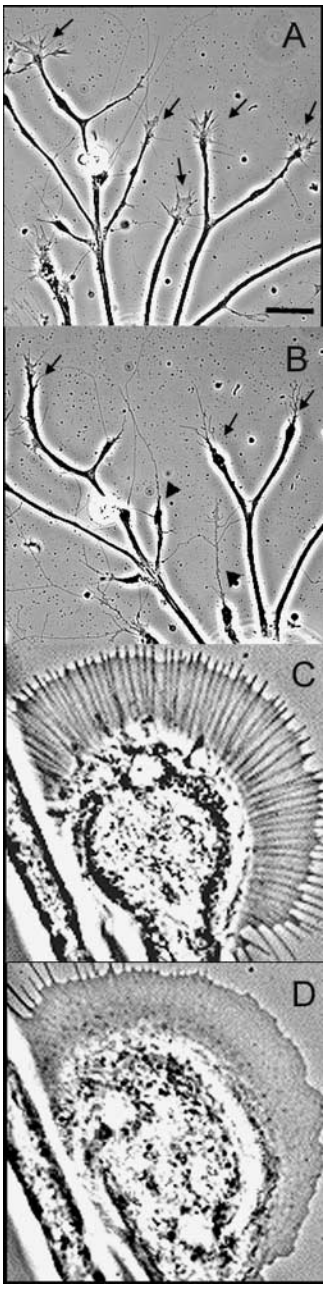

Figure 3. Phorbol ester TPA-induced growth cone collapse in CM correlates with actin bundle loss in PA growth cones. Similar to ML-7, PKC activator TPA caused CM growth cone collapse (B, arrows) and neurite retraction (arrowheads) compared with before application (A). When TPA was applied to PA growth cones (C), it caused actin bundle loss (D). Bar: (A and B) 20 μm; (C and D) 5 μm.

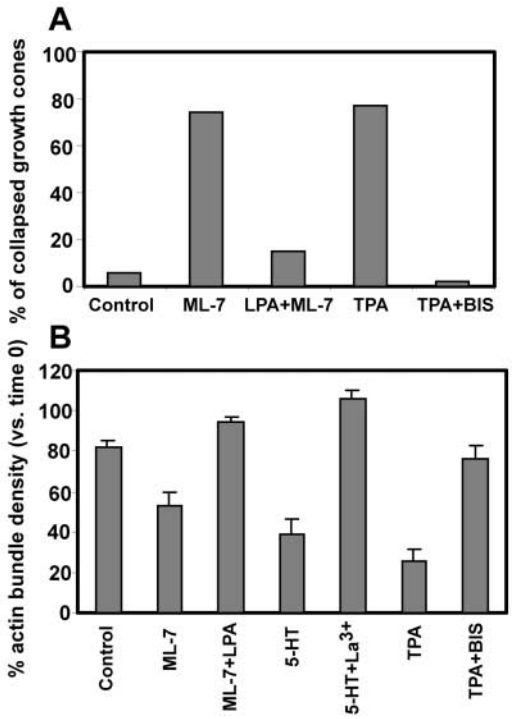

Figure 4. Treatments that inhibit growth cone collapse in CM also inhibit actin bundle loss in PA growth cones. (A) Growth cones in CM were exposed to either 5 μM ML-7 or 100 nM TPA for 30 min. Both ML-7 ($n = 77$) and TPA ($n = 96$) caused significant growth cone collapse compared with the control ($n = 100$, $P < 0.0001$). Pretreating growth cones with LPA antagonized ML-7–induced growth cone collapse ($n = 88$, $P < 0.0001$), whereas pretreatment with PKC inhibitor BIS inhibited TPA-induced growth cone collapse ($n = 111$, $P < 0.0001$). (B) Pretreating PA growth cones with La^{3+} ($n = 10$, $P < 0.0001$), LPA ($n = 13$, $P < 0.0001$), and BIS ($n = 24$, $P < 0.0001$) antagonized serotonin- ($n = 17$), ML-7– ($n = 17$), and TPA- ($n = 25$) induced actin bundle loss (after 1 h), respectively.

control condition. The actin filaments in the P-domain of the growth cone were mainly composed of two structures, radially arranged actin bundles and actin meshwork between the bundles that accumulates near the leading edge (Fig. 5, inset). After treatment with serotonin, ML-7, and TPA, growth cones were stained and their actin reorganization was observed. PA growth cones treated with serotonin, ML-7, and TPA all had fewer actin bundles but still retained a prominent actin meshwork (Fig. 5, B–D), indicating specific effects of these collapsing factors on actin bundle loss. In control growth cones, actin filaments are usually concentrated at the leading edge and in actin bundles (Fig. 6 A). After treatment with ML-7, we observed that, together with the actin bundle loss, the concentrated actin filaments at the leading edge of the growth cone also decreased dramatically, indicating decreased actin assembly. In addition, there appeared a dense arc-shaped actin structure (which we call an actin ring) located at the border of the growth cone central domain (Fig. 6 B). Similarly, both serotonin and TPA induced loss of F-actin accumulation at the leading edge and F-actin ring structures near the central domain (Fig. 6, C and D), indicating specific actin reorganization. Treating growth cones with BDM also resulted in loss of actin bundles. When these growth cones were stained with phalloidin, they also lost actin accumulation at the leading edge. However, there was no actin accumulation near the central domain (Fig. 6 F). Because BDM is a general myosin inhibitor that inhibits actin retrograde flow, this suggests that the ring structure is probably the consequence of interaction between dissociated actin meshwork powered by retrograde flow and the dense mass (microtubules and organelles) in the central domain. The fluorescent density profiles, which represent the actin filament distribution in growth cones (Fig. 6 G), showed that ML-7, serotonin, and TPA all caused a specific redistribution of intact actin filaments away from the leading edge towards the central domain. This actin filament redistribution has also been observed when growth cones are challenged with thrombin (de La

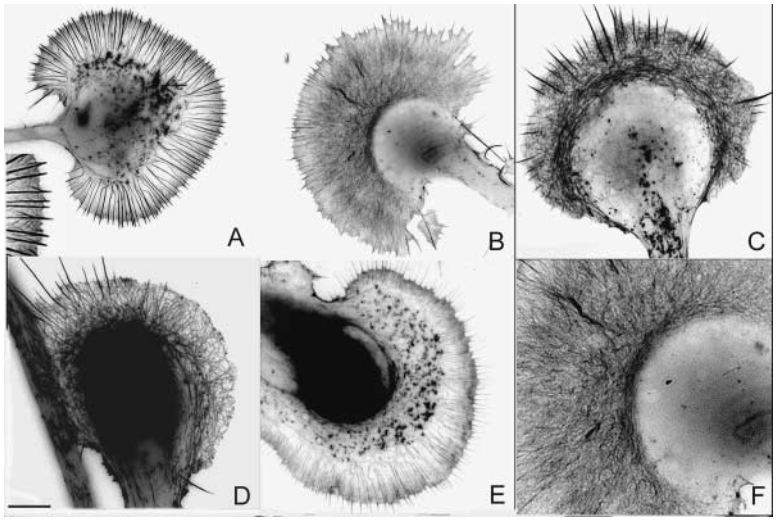

Figure 5. Serotonin, ML-7, and TPA induce actin reorganization from bundled structure to meshwork structure of PA growth cones. Intensity values of fluorescence images were inverted to show filamentous structure more clearly. Actin filaments in a control growth cone (A) are organized into two structures, radially arranged actin bundles and actin meshwork between bundles (inset). F-actin reorganized from bundled structure to meshwork after treatment with ML-7 (B), serotonin (C), and TPA (D). Treating growth cones with 0.1 μM cytochalasin induced general actin disassembly with increased actin aggregates around the central domain (E). High magnification of actin organization in ML-7–treated growth cones indicates F-actin around the C-domain rather than actin aggregates seen in cytochalasin-treated growth cones (F). Bar: (A–E) 10 μm; (F) 5 μm.

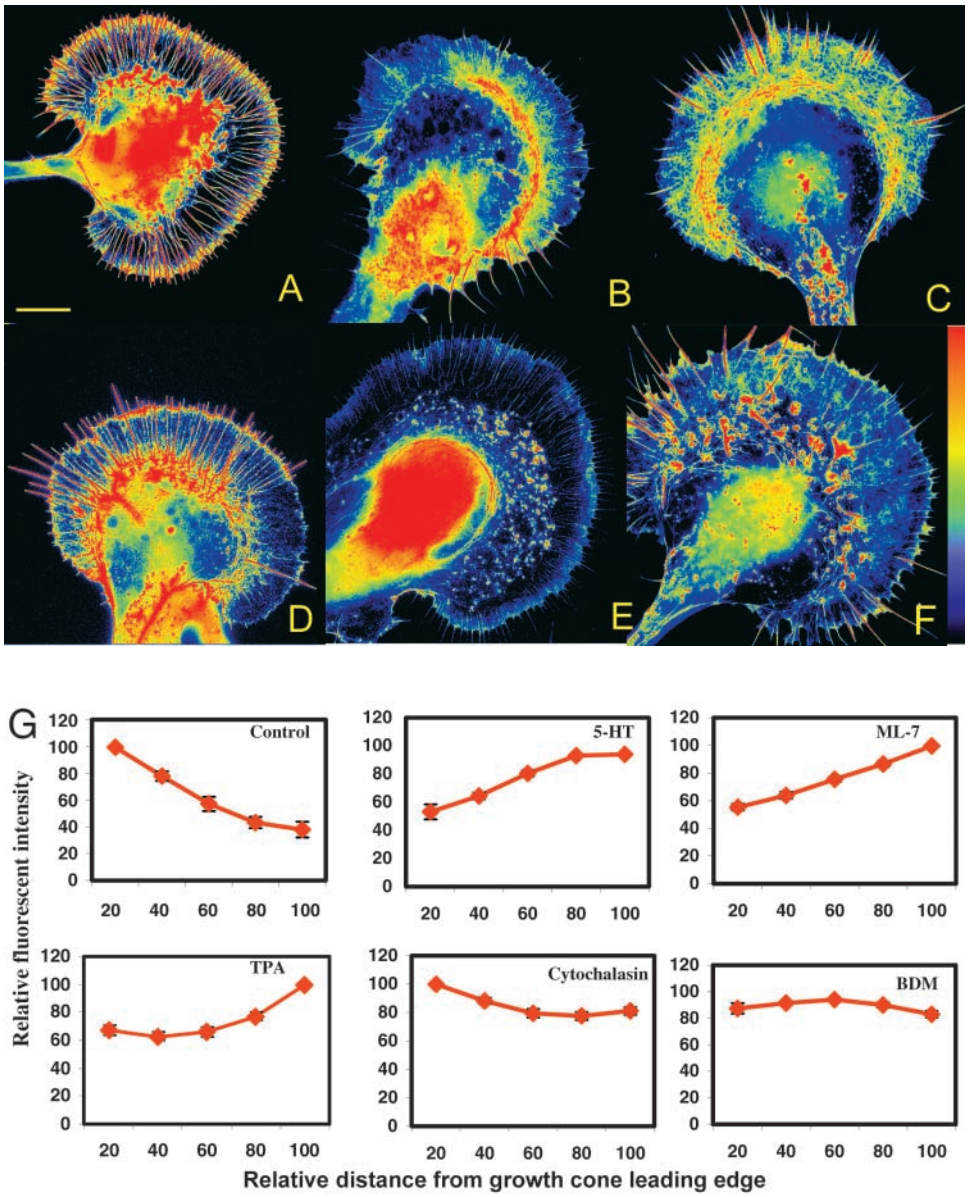

Figure 6. Serotonin, ML-7, and TPA induce actin filament redistribution away from the growth cone leading edge towards the center. Pseudocolor images transformed the intensity of bodipy FL phallacidin fluorescence to the color scale shown in the spectrum bar, with red indicating high intensity. In control growth cones (A), actin filaments are concentrated at the leading edge. When PA growth cones were exposed to ML-7 (B), serotonin (C), and TPA (D), actin accumulation at the leading edge decreased after actin bundle loss. In the meantime, there appeared to be accumulation of actin filaments near the center of growth cones. However, treating growth cones with low concentration of cytochalasin did not mimic the effects of the three collapsing factors. There is still a relatively higher concentration of actin at the leading edge after cytochalasin treatment (E). General myosin inhibitor BDM induced loss of actin accumulation at the leading edge without translocation to the C-domain (F). (G) Fluorescent intensity profiles from the leading edge to the C-domain indicate that compared with control (n = 7) only ML-7 (n = 14), serotonin (n = 8), and TPA (n = 8) induced actin filament redistribution from the leading edge to the center of growth cones. Both cytochalasin (n = 9) and BDM (n = 7) did not induce similar actin redistribution. Bar, 10 μm.

Houssaye et al., 1999) and during AL-1–induced growth cone collapse (Meima et al., 1997). As a control, we also treated growth cones with cytochalasin D, an inhibitor of actin polymerization. Low concentration (0.1 μM) cytochalasin has been used to specifically reduce growth cone actin bundles (Challacombe et al., 1996). Although 0.1 μM cytochalasin D diminished actin bundles when observed using phase–contrast microscopy, stained growth cones still exhibited both actin bundle and meshwork structures but with reduced F-actin concentration (Fig. 5 E). In addition, there were increased F-actin aggregates found adjacent to the central domain (C-domain) of cytochalasin-treated growth cones (Fig. 5 E), which suggests an increase in disassembly or severing of actin filaments. This is consistent with the role of cytochalasin as a general F-actin disorganization agent. Fig. 5 F provides more details of the actin structure close to the C-domain of ML-7–treated growth cones. It shows clearly that actin near the central domain was intact F-actin meshwork, which was significantly different from actin aggregates shown in cytochalasin-treated growth cones. Confocal microscopic study also showed similar results (data not shown). Moreover, growth cones treated with cytochalasin still had relatively higher F-actin concentration at the leading edge (Fig. 6 E). Together, our results showed that all three collapsing factors caused specific actin bundle loss. It coincided with decreased actin assembly at the leading edge and reorganization of actin meshwork that was not mimicked by cytochalasin.

Actin Bundle Loss Parallels Growth Cone Collapse

We have shown a clear correlation between collapse of CM growth cones and actin bundle loss in PA growth cones, which suggests that actin bundles play a critical role in maintaining growth cone morphology. However, we cannot rule out the possibility that CM and PA growth cones may respond to collapsing factors through different pathways due to different culture conditions in addition to the difference in substrate adhesion. Fortunately, we were able to find some larger CM growth cones in which actin bundles were more prominent and which collapsed more slowly than smaller CM growth cones. These growth cones emerge from the cell body, grow, turn, and collapse in response to collapsing factors, which is characteristic of all CM growth cones. By taking time-lapse movies of these growth cones upon application of collapsing factors, we were able to show actin bundle loss and growth cone collapse simultaneously in the same growth cones. Fig. 7, A–D, shows how such a growth cone responded to ML-7 application. After the growth cone contacted ML-7 released from a pipette, actin bundle loss occurred before significant growth cone collapse. Quantitative data showed that actin bundle loss was significantly faster at the beginning, and then the decrease rate of actin bundle number was parallel to the decrease of growth cone lamellipodia surface area (Fig. 7 K). Moreover, similar to PA growth cones, LPA pretreatment antagonized both actin bundle loss and lamellipodia retraction (Fig. 7 K). Collapsed growth cones recovered quickly after the pipette was removed (Fig. 7 E), which was similar to smaller CM growth cones shown above (Fig. 2 C). In control growth cones, both actin bundle number and lamellipodia area remained constant (Fig. 7 J). To show actin reorganization in CM growth cones, we fixed and stained growth cones after actin bundle loss but before complete collapse (Fig. 7, G and H). Results showed that there was also loss of actin accumulation from the leading edge and actin translocation to the central domain (Fig. 7 I), whereas control growth cones showed similar actin accumulation at the leading edge to that of PA growth cones (Fig. 7 F). This indicates that CM growth cones share similar responses to collapsing factors to that of PA growth cones.

Extension of actin bundles from a severed axonal stump is the first step of growth cone morphogenesis, followed by lamellipodia protrusion to form the growth cone (Goldberg and Wu, 1995; Welnhofer et al., 1997). When axons were cut in the presence of a collapsing factor (ML-7, 50 μM), the formation of actin bundles was significantly inhibited, which blocked PA growth cone formation (20.7%, n =29 vs. 95%, n = 22 in control). Similarly, this inhibition was rescued by LPA pretreatment (90%, n = 30). Moreover, challenging newly formed PA growth cones (30 min after axotomy, which have less surface area and therefore less adhesion to the substrate) with ML-7 also caused growth cone collapse (34.8%, n = 23 vs. 0% of control, n = 16) that was antagonized by LPA (13.6%, n = 22), indicating a similar response to that of CM growth cones. Together, this suggests that actin bundles are required for both maintenance and formation of growth cone morphology. Thus, actin bundle loss and coincident decrease of actin accumulation at the leading edge could be the underlying mechanism of growth cone collapse upon contacting collapsing factors.

Collapsing Factor–induced Actin Reorganization Is Not Due to Direct Inhibition of Actin Polymerization

The inability of cytochalasin to mimic effects of collapsing factors on actin reorganization suggests that collapsing factors induce a decrease of actin accumulation at the leading edge in a different way than cytochalasin. Therefore, we directly tested whether collapsing factors inhibit actin polymerization. It has been shown that the retrograde flow in growth cones is powered by myosin, and treating the growth cone with BDM, a general myosin ATPase inhibitor, attenuates retrograde flow (Lin et al., 1996). This also results in filopodia lengthening due to actin polymerization in the absence of retrograde flow, and this effect is inhibited by cytochalasin (Lin et al., 1996; Mallavarapu and Mitchison, 1999). Thus, BDM-induced filopodia lengthening was used as an assay for actin polymerization. To examine whether collapsing factors affected this actin polymerization, we treated PA growth cones either with BDM alone or with both BDM and collapsing factors. We then measured the filopodia elongation rate and the change of filopodia length under both conditions. The results showed no significant decrease between the groups (Fig. 8, A and B), indicating that ML-7, serotonin, and TPA do not decrease actin polymerization. On the contrary, serotonin caused faster filopodia lengthening than BDM alone. This is because calcium influx alone caused by serotonin can induce an increase of actin polymerization at filopodia tips (Welnhofer et al., 1999). These re-

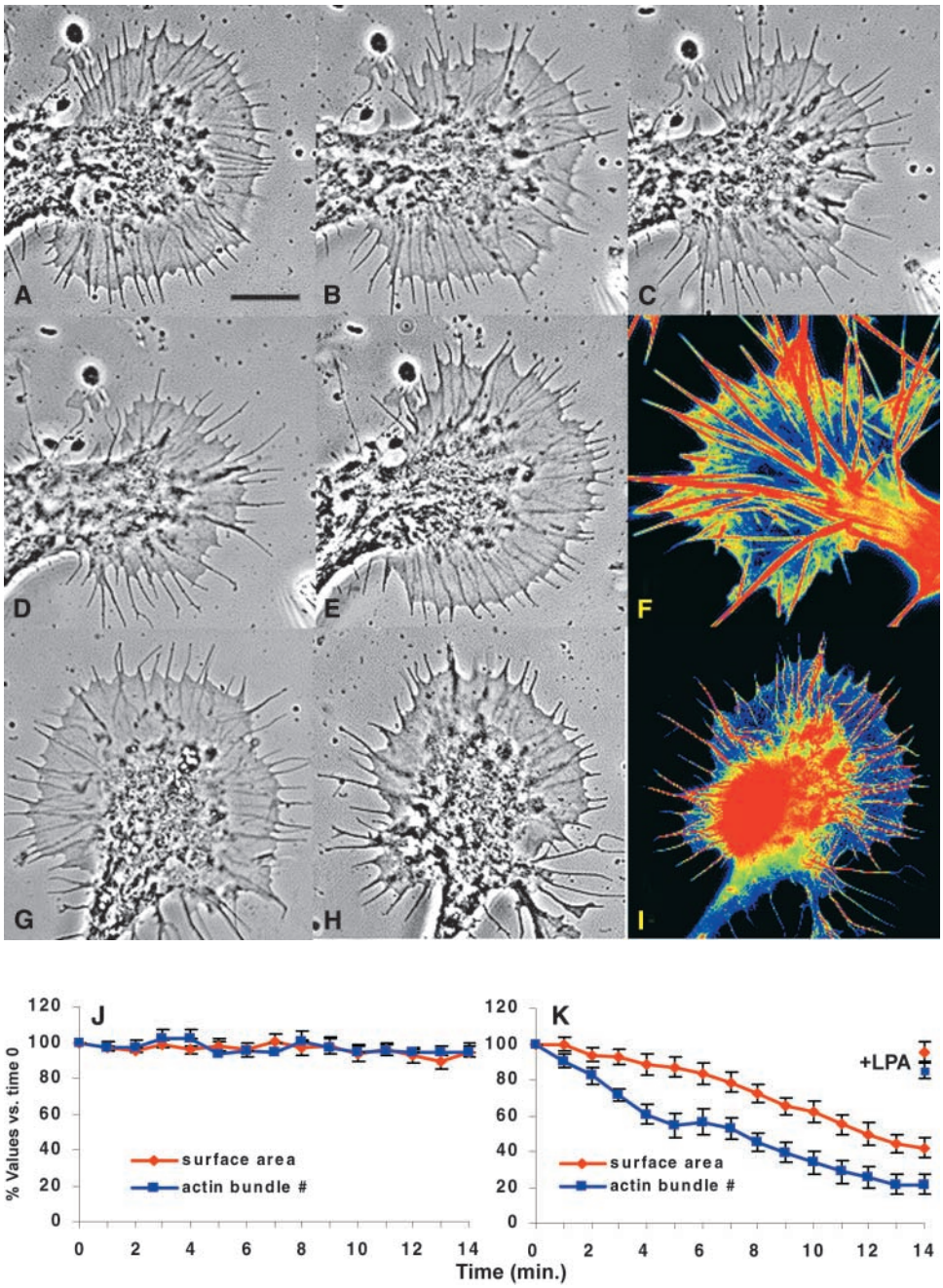

Figure 7. Decrease of actin bundles parallels collapse in extending CM growth cones. Larger motile CM growth cones have prominent actin bundles (A). When these growth cones were treated with ML-7, the number of actin bundles decreased dramatically before significant lamellipodia retraction occurred (B). Continuous exposure to ML-7 caused further decrease of actin bundles and coincident lamellipodia retraction (C and D). Growth cone morphology recovered after ML-7 was removed (E). Similar to PA growth cones, control CM growth cones have actin accumulation at the leading edge (F, same pseudocolor rendering as above). Growth cones treated with ML-7 were fixed after they started to lose actin bundles but before their total collapse (G and H). Actin staining showed loss of actin accumulation from the leading edge and translocation of actin to the central domain (I). The decease rates of actin bundles and lamellipodia surface area were measured and presented as a percentage value compared with time zero. In the control, both actin bundle number and lamellipodia surface area remained constant (J, $n = 6$). In ML-7–treated growth cones, the decrease of actin bundle number was faster at the beginning and then paralleled changes of lamellipodia surface area (K, $n = 8$). LPA pretreatment antagonized both actin bundle loss and growth cone collapse ($n = 13$). Note that only a single time point (14 min) is shown for LPA effect. Bar, 10 μm.

sults further confirm that direct inhibition of actin polymerization is unlikely the primary cause of effects induced by serotonin, ML-7, and TPA. Moreover, preincubating growth cones with phalloidin did not block ML-7–induced actin bundle loss (29.62 ± 11.05%, $P < 0.0001$ compared with control). This is consistent with our previous study showing that phalloidin also had little protective effect against actin bundle dissociation caused by calcium influx (Welnhofer et al., 1999). Together, these results indicate that the serotonin, ML-7, and TPA induce the loss of actin bundles and actin accumulation at the leading edge mainly through reorganization of actin filaments but not direct inhibition of F-actin assembly in a way similar to cytochalasin.

Three Collapsing Factors Induce Actin Bundle Loss through Different Pathways

Even though ML-7 is a specific inhibitor of MLCK (K_i = 0.3 μM), it also inhibits PKA and PKC but at much higher concentrations (K_i = 21 and 42 μM, respectively). To ascertain if the effect of ML-7 on PA growth cones was due to its inhibition of MLCK rather than other kinases, various kinase inhibitors were tested, including WT (K_i = 0.2 μM for MLCK, K_i = 5 nM for phosphatidylinositol 3-kinase), H-7 (K_i = 6 and 3 μM for PKC and PKA, respectively, versus K_i = 97 μM for MLCK), PKA-specific inhibitor KT-5720 (K_i = 56 nM), PKC-specific inhibitor BIS (K_i = 10 nM), and general kinase inhibitor staurosporine (K_i = 1.8 nM for MLCK). Results are shown in Fig. 9

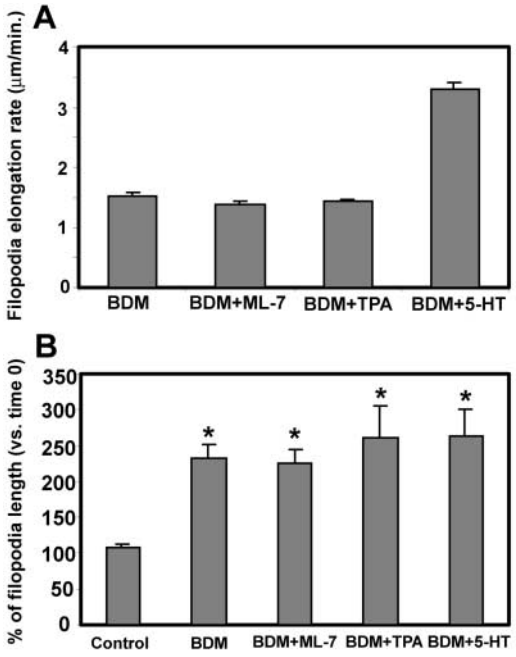

Figure 8. Serotonin, ML-7, and TPA do not decrease actin polymerization in vivo. When growth cones are treated with BDM, a general myosin inhibitor, filopodia elongation occurs via actin polymerization during inhibition of retrograde flow. (A) Filopodia elongation rates were measured after growth cones were treated with BDM (10 mM, $n = 113$), BDM plus ML-7 ($n = 72$), BDM plus serotonin ($n = 64$), and BDM plus TPA ($n = 73$). The control rate was considered zero because no filopodia in control growth cones can be found that elongates continuously for four frames. Note the absence of any inhibiting effect on BDM-induced filopodia elongation rate. (B) Filopodia length changes were measured after 10 min without treatment ($n = 15$, growth cones) or with BDM ($n = 12$, growth cones), BDM plus ML-7 ($n = 13$, growth cones), BDM plus TPA ($n = 9$, growth cones), and BDM plus 5-HT ($n = 10$ growth cones). Similarly, none of the treatments inhibited the filopodia elongation induced by BDM. *Significant difference from the control.

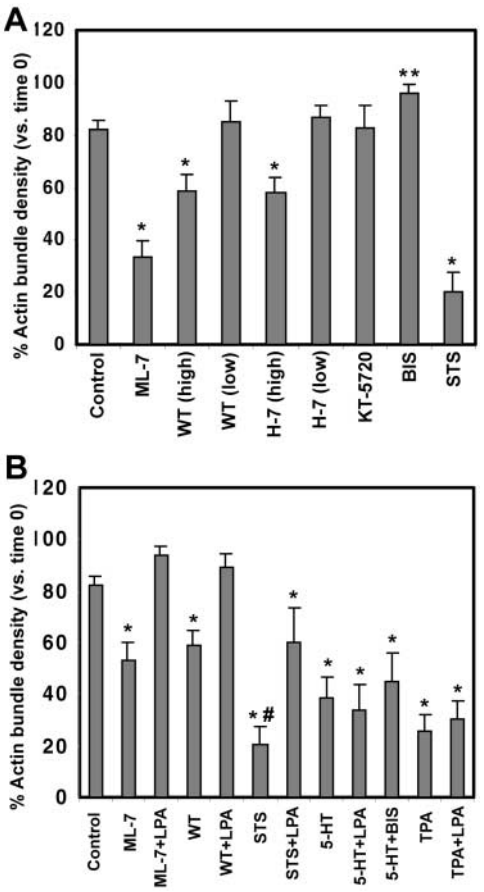

Figure 9. ML-7, serotonin, and TPA induce actin bundle loss through different signal pathways. (A) ML-7 induces actin bundle loss through inhibition of MLCK. In addition to ML-7 (10 μM, $n = 24$), several kinase inhibitors were tested (1-h treatment), including WT (10 μM, $n = 19$; 200 nM, $n = 11$), H-7 (500 μM, $n = 11$; 100 μM, $n = 20$), KT-5720 (1 μM, $n = 16$), BIS (200 nM, $n = 17$), and STS (5 nM, $n = 11$). Note that only agents inhibiting MLCK activity induced significant actin bundle loss compared with the control ($n = 38$). (B) Serotonin and TPA induce actin bundle loss through different pathways than ML-7. In addition to ML-7, LPA treatment also inhibited WT- ($n = 26$) and STS- ($n = 11$) induced actin bundle loss (after 1 h). However, it had no effect on either serotonin- ($n = 16$) or TPA- ($n = 15$) induced actin bundle loss. In addition, PKC inhibitor BIS ($n = 14$) had no effect on serotonin-induced actin bundle loss. $*P < 0.0005$, significant difference from the control; $**P < 0.05$; $\#P < 0.05$, significant difference from STS plus LPA.

A. In summary, the concentration of H-7 necessary to cause actin bundle loss was substantially higher than that needed to inhibit PKA and PKC. WT, which inhibits MLCK via a different mechanism from ML-7, caused actin bundle loss only at micromolar concentration. In addition, PKA- and PKC-specific inhibitors had little effect at high concentrations. Finally, our results showed that LPA antagonized actin bundle loss induced by ML-7, WT, and staurosporine (Fig. 9 B). Together, our findings suggest that the actin bundle loss caused by ML-7 was likely due to its inhibition of MLCK and subsequent myosin II inhibition, which is antagonized by LPA treatment. We also tested whether serotonin and TPA induced actin bundle loss through different signal transduction pathways from ML-7. First, we tested whether LPA pretreatment had any effect on either serotonin- or TPA-induced actin bundle loss. Our results showed that LPA prevented neither TPA- nor serotonin-induced effects on actin bundles (Fig. 9 B). Second, because calcium can also activate PKC we examined whether PKC inhibitor antagonized the effect of serotonin. We found that PKC inhibitor BIS had little effect on serotonin-induced actin bundle loss (Fig. 9 B). Taken together, it is very likely that serotonin and TPA each induces growth cone actin bundle loss through different signal pathways, which are both different from that of ML-7.

Discussion

Use of the Helisoma Model in Studying Growth Cone Collapse

The model we used in our study is *Helisoma* ganglion neurons. When these neurons are cultured in CM that contains growth factors and extracellular matrix proteins, they

grow neurites with motile growth cones at the tip. These growth cones share similar morphology and motility to vertebrate growth cones (compare to Paglini et al., 1998). When these neurons are plated onto polylysine-coated coverslips, they form a larger nonmotile growth cone. Because of the high adhesion of the growth cone membrane to the substrate, the growth cone on polylysine does not collapse even when the actin filaments, which support the growth cone structure, are completely depleted by cytochalasin. This property allowed us to observe the cytoskeletal reorganization process when growth cones respond to collapsing factors in the absence of growth cone collapse. As a result, we can dissect the initial cytoskeletal events that mediate the collapse, which normally occurs very quickly and is followed by dramatic morphological change and membrane retraction. Previous studies have shown that *Helisoma* PA and CM growth cones share similar properties, including both morphological and cytoskeletal features and responses to neurotransmitters (Williams and Cohan, 1994). Thus, it is reasonable to hypothesize that growth cones cultured in both conditions also share similar cytoskeletal events in response to extracellular factors. By studying the cytoskeletal rearrangement in larger nonmotile PA growth cones, we could test the cytoskeletal mechanisms underlying the collapse of growth cones cultured in CM. Furthermore, after identifying the cytoskeletal changes induced by collapsing factors in PA growth cones it was possible to verify the same changes in CM growth cones, bringing both findings together in one condition. When using pharmacological kinase inhibitors in the studies, we assumed that the K_i values of these inhibitors for *Helisoma* kinases were similar to those of vertebrates, although they were not tested directly.

Effects of F-Actin Reorganization during Growth Cone Collapse

We demonstrate for the first time that actin bundle loss is correlated with growth cone collapse. First, collapsing factors that induce actin bundle loss from PA growth cones cause collapse of growth cones of the same neurons in CM. Second, treatments that prevent actin bundle loss also antagonize growth cone collapse. Third, actin bundle loss also coincides with loss of actin accumulation from the leading edge, which is characteristic of actin reorganization during growth cone collapse (Fan et al., 1993; Meima et al., 1997). Fourth, formation of actin bundles is required for growth cone morphogenesis. Finally, loss of actin bundles parallels collapse of extending CM growth cones. Together, our data show that actin bundle loss is both necessary and sufficient for CM growth cone collapse, suggesting it as an underlying mechanism of growth cone collapse.

Why does actin bundle loss induce growth cone collapse? To answer this question, we need to know what is required to maintain the growth cone morphology. First, as suggested by many studies, the growth cone leading edge is determined by the balance between actin polymerization and retrograde actin flow (Mallavarapu and Mitchison, 1999). Thus, there must be efficient actin assembly at the leading edge to balance the retrograde flow that moves actin filaments away from the leading edge. Second, the growth cone cytoskeleton must attach to the substratum through focal contacts. It is possible that actin bundle structure contributes to both processes.

Actin filaments are usually concentrated at the leading edge of growth cones (Bentley and O'Connor, 1994; Fig. 6 A and Fig. 7 F). It has been shown that F-actin is relatively concentrated at the leading edge of lamellipodia that are advancing and reduced in places that are retracting (O'Connor and Bentley, 1993). When the growth cone contacts with collapsin, a repulsive factor that causes growth cone collapse (Luo et al., 1995), the concentration of F-actin at the leading edge decreases dramatically (Fan et al., 1993). This phenomenon was also observed in myelin-induced growth cone collapse (Kuhn et al., 1999). In our results, upon actin bundle loss by collapsing factors the accumulation of F-actin at the leading edge decreased dramatically, indicating decreased actin assembly at the leading edge. This coincident loss of actin bundles and F-actin at the leading edge suggests that actin bundles play a unique role in regulating actin assembly at the leading edge. One possibility that actin bundles help actin accumulation at the leading edge is that organizing actin filaments into ordered bundles leads to smaller tilt angles between filaments at the leading edge and the direction of retrograde flow. As a result, this enhances the efficiency of actin assembly versus retrograde flow and leads to actin accumulation at the leading edge (Danuser and Oldenbourg, 2000). Therefore, dissociation of actin bundles by collapsing factors may increase tilt angles of filaments at the leading edge, which then leads to decrease of actin accumulation at the leading edge and lamellipodia retraction due to retrograde flow. Another possibility is that actin-bundling proteins inhibited by collapsing factors are directly involved in regulating actin assembly. For instance, a dictyostelium actin-bundling protein can inhibit actin disassembly (Zigmond et al., 1992), and α-actinin is able to increase F-actin end number and the subsequent actin polymerization (Colombo et al., 1993). The third possibility is direct inhibition of actin polymerization in a way similar to that of cytochalasin. However, according to our results this is unlikely (see discussion below).

Actin bundles may also help anchor the growth cone to the substratum by forming focal contacts. Izzard and Lochner (1980) have shown that formation of the focal contacts is preceded by the development of a microspike (actin bundles). Moreover, they also show that the formation of focal contacts plays a primary role in lamellipodia spreading. In addition, study of growth cones with interference reflection microscopy shows that filopodia and their associated actin bundles are much closer to the substratum than lamellipodia between them (Letourneau, 1979). Therefore, loss of actin bundles may lead to loss of focal contacts and subsequent lamellipodia retraction, namely, growth cone collapse. This is supported by the result that inhibition of ezrin/radixin/moesin (ERM) proteins, which are important for stress fiber and focal adhesion formation through cross-linking F-actin and plasma membranes (Mackay et al., 1997), in vertebrate growth cones leads to strikingly similar changes to our results: actin bundle loss and growth cone collapse (Paglini et al., 1998). In addition, phorbolester PMA arrests neurite outgrowth and growth cone motility through perturbing actin bundles and the formation of substratum attachment sites (Muir et al., 1989).

Collapsing Factors Do Not Directly Inhibit Actin Polymerization

F-actin rearrangement in growth cones upon collapse has been thought to be similar to cytochalasin-induced changes (Fan et al., 1993; Meima et al., 1997), which are based on direct inhibition of actin polymerization at barbed ends. However, our results showed that cytochalasin was unable to mimic the effects of collapsing factors on growth cone actin reorganization. First, growth cones treated with collapsing factors lack actin bundles but still have prominent actin meshwork. Considering that retrograde flow continues after actin bundle loss (data not shown), this indicates actin polymerization still occurs. On the contrary, cytochalasin causes retraction of actin filaments away from the leading edge that ultimately leads to a complete loss of F-actin as retrograde flow continues without actin polymerization (Lin et al., 1996). Second, our data show that all three collapsing factors did not decrease actin polymerization in vivo. Third, our results show that growth cones treated with low concentration of cytochalasin still have a relatively higher concentration of actin filaments at the leading edge (Fig. 6 E). In addition, there is no translocation of actin filaments to the center of the growth cone. Cytochalasin also induces an increase of actin aggregates near the C-domain (Fig. 5 E), which is consistent with its role of actin disassembly. Thus, collapsing factor–mediated growth cone collapse probably involves coordinated cytoskeletal rearrangement mediated by actin bundles, whereas cytochalasin only causes general F-actin disorganization. Our results are consistent with the study by Fournier et al. (2000), which aruges cytochalasin failed to mimic morphological changes induced by collapsing factors. This suggests an alternative pathway to decrease actin assembly at the growth cone leading edge after contacting collapsing factors. However, net loss of F-actin may occur later due to drastic growth cone morphological change and membrane retraction. Furthermore, our recent data show that collapsing factor–induced F-actin reorganization correlates with inhibition of microtubule dynamic ends into growth cone P-domain (data not shown), whereas cytochalasin enhances protrusion of microtubule ends into the P-domain (Forscher and Smith, 1988). Taken together, our results suggest that growth cone collapse, or at least the initiation of collapse, may be mainly a process involving F-actin reorganization that results in decreased actin assembly at the leading edge rather than direct inhibition of actin polymerization.

Actin Bundle Loss Is a Converging Cytoskeletal Mechanism of Different Growth Cone Collapsing Pathways

Growth cone collapse is induced by a variety of stimuli. Our results indicate that three collapsing factors tested here may induce growth cone collapse by affecting actin bundling through different signal transduction pathways (Fig. 10). First, our kinase inhibition results indicate that inhibition of MLCK is likely the cause behind actin bundle loss induced by ML-7 that is consistent with the study by Jian et al. (1994). Since the only target of MLCK is myosin light chain that is essential for myosin II activation (Bresnick, 1999), this implies that myosin II is very likely involved in ML-7–induced growth cone collapse and actin bundle loss. Indeed, myosin II may organize actin filaments into bundles (Rochlin et al., 1995; Verkhovsky et al., 1995). Moreover, LPA, which can activate Rho and subsequent myosin light chain (Kimura et al., 1996), antagonized the effects of three different MLCK inhibitors. This further implies the involvement of myosin II inhibition in ML-7–induced effects. Our results are consistent with the study by Jin and Strittmatter (1997), which shows active Rho is required to maintain spread growth cone morphology and results from Kuhn et al. (1999) and that Rho activation antagonizes myelin-induced growth cone collapse. However, the role of Rho and myosin II in regulating growth cone motility is at best controversial. Growth cones of N1E-115 neuroblastoma cells collapse and retract if treated with LPA, probably through activation of Rho and subsequent myosin II (Kozma et al., 1997; Amano et al., 1998). One possible explanation for this inconsistency, as suggested by Sebok et al. (1999), is the differential state and properties of the model systems used. They showed that activation of Rho prevented neurite outgrowth from undifferentiated PC12 cells, but it induced significant neurite extension in NGF-primed and -differentiating cells. In addition, activation of Rho in mature primary cultured neurons only has a minor effect on axon elongation that is in sharp contrast to the case in neuronal cell lines (Bito et al., 2000). Another possibility is that ERM proteins, which link actin bundles to membrane proteins (Mangeat et al., 1999), are also regulated by Rho and myosin phosphatase (Fukata et al., 1998). Therefore, activation of ERM proteins by LPA might antagonize actin bundle dissociation and growth cone collapse caused by MLCK inhibition.

The second evidence for different signaling pathways is that calcium influx is considered to be the mechanism of serotonin-induced growth cone collapse and actin bundle loss (Cohan et al., 1987). Thus, calcium-regulated actin-bundling proteins may be involved in mediating the serotonin effects, such as α-actinin (Noegel et al., 1987) and fimbrin (de Arruda et al., 1990). This may also be true for semaphorin 3A (Behar et al., 1999) and neurite outgrowth inhibitor NI-35–induced growth cone collapse (Bandtlow et al., 1993), which both require calcium influx.

The third evidence is that the antagonizing effect of specific PKC inhibitor against TPA effects indicates the requirement of PKC. One possible target of PKC is fascin, an actin-bundling protein that is inactivated by PKC phosphorylation (Yamakita et al., 1996). This is supported by our observation that fascin colocalizes with actin bundles in *Helisoma* growth cones (Cohan et al., 2001). Downregulation of fascin expression in neurons results in growth cone collapse (Edwards and Bryan, 1995), which strongly supports our conclusion that actin bundles play an important role in maintaining growth cone morphology. Moreover, recently identified Ena/VASP proteins that may function downstream of guidance signals, such as Netrin/DCC and Slit/Robo, are also actin-bundling proteins (Bachmann et al., 1999; Lanier and Gertler, 2000). They localize mainly to the tips of filopodia (Lanier et al., 1999) where fascin is also concentrated (Cohan et al., 2001). Finally, serotonin, ML-7, and TPA induced actin bundle loss by regulating different aspects of actin dynamics. ML-7 causes actin bundle decrease by merging adjacent bundles

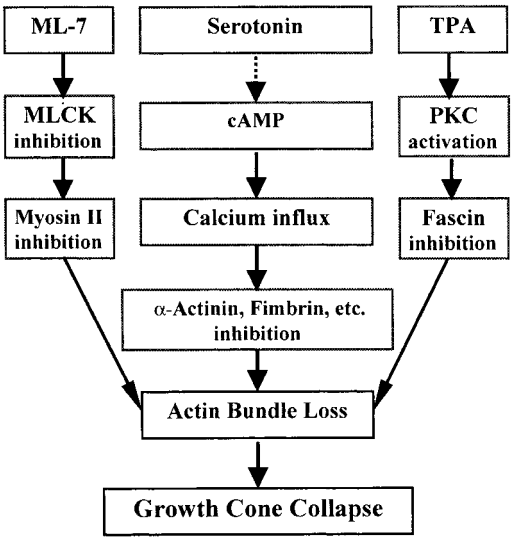

Figure 10. Proposed model illustrating signaling pathways that mediate the growth cone collapse through actin bundle loss. Myosin II is the likely target for ML-7–induced growth cone collapse. Myosin II can organize actin filaments into bundles, and its inhibition causes growth cone collapse. Consistent with this, antisense oligo DNA complementary to a specific isoform of conventional myosin (myosin IIB) attenuates growth cone motility and neurite growth (Wylie et al., 1998). Calcium influx has been shown to mediate serotonin-induced growth cone collapse and NI-35 and collapsin. It may induce collapse via actin bundle loss by changing calcium-regulated actin-bundling proteins such as α-actinin and frimbrin. One potential target that mediates PKC-induced growth cone collapse is fascin, an actin bundling protein localized in *Helisoma* growth cones. Phosphorylation of fascin by PKC inhibits its ability to bind actin filaments and induces actin bundle dissociation. Inhibition of fascin expression alone in neurons can cause growth cone collapse.

through lateral flow which leads to fewer but thicker bundles (data not shown). Calcium influx induces dissociation of actin bundles resulting in thinner bundles and filopodia elongation (Welnhofer et al., 1999), whereas TPA causes faster bundle dissociation without filopodia lengthening (Cohan et al., 2001).

In summary, in this study we observed that serotonin, ML-7, and TPA all induce similar actin bundle loss and associated actin reorganization correlated with growth cone collapse. In addition, Ca^{2+} and PKC are both common downstream signaling factors of a wide variety of extracellular guidance cues. Thus, our study suggests that actin bundle loss may be a common cytoskeletal event when growth cones respond to physiological collapsing cues that use calcium/PKC/MLCK (myosin II) as downstream signals. Indeed, it is more reasonable to hypothesize that different guidance cues converge into common cytoskeletal events that may be regulated by different molecules. Therefore, our observations not only suggest a potential common cytoskeletal mechanism of growth cone collapse but also help us to further understand how guidance cues are translated into cytoskeletal rearrangement and directed neurite growth by defining potential candidates downstream of growth cone collapsing cues that act on actin bundles.

The authors are grateful to Dr. John Kolega for his comments on this manuscript.

This work was supported by grants from the National Institutes of Health (NS25789) and National Science Foundation (IBN 0082793) to C.S. Cohan, and by funds from the Mark Diamond Research Fund of the Graduate Student Association at the State University of New York to F.-Q. Zhou.

Submitted: 28 November 2000
Revised: 13 April 2001
Accepted: 13 April 2001

References

Amano, M., M. Ito, K. Kimura, Y. Fukata, K. Chihara, T. Nakano, Y. Matsuura, and K. Kaibuchi. 1996. Phosphorylation and activation of myosin by Rho-associated kinase (Rho-kinase). *J. Biol. Chem.* 271:20246–20249.

Amano, M., K. Chihara, N. Nakamura, Y. Fukata, T. Yano, M. Shibata, M. Ikebe, and K. Kaibuchi. 1998. Myosin II activation promotes neurite retraction during the action of Rho and Rho-kinase. *Genes Cells.* 3:177–188.

Bachmann, C., L. Fischer, U. Walter, and M. Reinhard. 1999. The EVH2 domain of the vasodilator-stimulated phosphoprotein mediates tetramerization, F-actin binding, and actin bundle formation. *J. Biol. Chem.* 274:23549–23557.

Bandtlow, C.E., M.F. Schmidt, T.D. Hassinger, M.E. Schwab, and S.B. Kater. 1993. Role of intracellular calcium in NI-35-evoked collapse of neuronal growth cones. *Science.* 259:80–83.

Behar, O., K. Mizuno, M. Badminton, and C.J. Woolf. 1999. Semaphorin 3A growth cone collapse requires a sequence homologous to tarantula hanatoxin. *Proc. Natl. Acad. Sci. USA.* 96:13501–13505.

Bentley, D., and T.P. O'Connor. 1994. Cytoskeletal events in growth cone steering. *Curr. Opin. Neurobiol.* 4:43–48.

Bito, H., T. Furuyashiki, H. Ishihara, Y. Shibasaki, K. Ohashi, K. Mizuno, M. Maekawa, T. Ishizaki, and S. Narumiya. 2000. A critical role for a Rho-associated kinase, p160ROCK, in determining axon outgrowth in mammalian CNS neurons. *Neuron.* 26:431–441.

Bresnick, A.R. 1999. Molecular mechanisms of nonmuscle myosin-II regulation. *Curr. Opin. Cell Biol.* 11:26–33.

Budnik, V., C.F. Wu, and K. White. 1989. Altered branching of serotonin-containing neurons in *Drosophila* mutants unable to synthesize serotonin and dopamine. *J. Neurosci.* 9:2866–2877.

Challacombe, J.F., D.M. Snow, and P.C. Letourneau. 1996. Actin filament bundles are required for microtubule reorientation during growth cone turning to avoid an inhibitory guidance cue. *J. Cell Sci.* 109:2031–2040.

Chien, C.B., and W.A. Harris. 1996. Signal transduction in vertebrate growth cones navigating in vivo. *Perspect. Dev. Neurobiol.* 4:253–266.

Cohan, C.S., J.A. Connor, and S.B. Kater. 1987. Electrically and chemically mediated increases in intracellular calcium in neuronal growth cones. *J. Neurosci.* 7:3588–3599.

Cohan, C.S., E.A. Welnhofer, L. Zhao, F. Matsumura, and S. Yamashiro. 2001. Role of actin bundling protein fascin in growth cone morphogenesis: localization in filopodia and lamellipodia. *Cell Motil. Cytoskeleton.* 48:109–120.

Colombo, R., I. DalleDonne, and A. Milzani. 1993. Alpha-actinin increases actin filament end concentration by inhibiting annealing. *J. Mol. Biol.* 230: 1151–1158.

Cox, E.C., B. Muller, and F. Bonhoeffer. 1990. Axonal guidance in the chick visual system: posterior tectal membranes induce collapse of growth cones from the temporal retina. *Neuron.* 4:31–37.

Danuser, G., and R. Oldenbourg. 2000. Probing f-actin flow by tracking shape fluctuations of radial bundles in lamellipodia of motile cells. *Biophys. J.* 79: 191–201.

de Arruda, M.V., S. Watson, C.S. Lin, J. Leavitt, and P. Matsudaira. 1990. Fimbrin is a homologue of the cytoplasmic phosphoprotein plastin and has domains homologous with calmodulin and actin gelation proteins. *J. Cell Biol.* 111:1069–1079.

de La Houssaye, B.A., K. Mikule, D. Nikolic, and K.H. Pfenninger. 1999. Thrombin-induced growth cone collapse: involvement of phospholipase A(2) and eicosanoid generation. *J. Neurosci.* 19:10843–10855.

Edwards, R.A., and J. Bryan. 1995. Fascins, a family of actin bundling proteins. *Cell Motil. Cytoskeleton.* 32:1–9.

Fan, J., and J.A. Raper. 1995. Localized collapsing cues can steer growth cones without inducing their full collapse. *Neuron.* 14:263–274.

Fan, J., S.G. Mansfield, T. Redmond, P.R. Gordon-Weeks, and J.A. Raper. 1993. The organization of F-actin and microtubules in growth cones exposed to a brain-derived collapsing factor. *J. Cell Biol.* 121:867–878.

Forscher, P., and S.J. Smith. 1988. Actions of cytochalasins on the organization of actin filaments and microtubules in a neuronal growth cone. *J. Cell Biol.* 107:1505–1516.

Fournier, A.E., F. Nakamura, S. Kawamoto, Y. Goshima, R.G. Kalb, and S.M. Strittmatter. 2000. Semaphorin 3A enhances endocytosis at sites of receptor–F-actin colocalization during growth cone collapse. *J. Cell Biol.* 149:411–422.

Fukata, Y., K. Kimura, N. Oshiro, H. Saya, Y. Matsuura, and K. Kaibuchi. 1998.

Association of the myosin-binding subunit of myosin phosphatase and moesin: dual regulation of moesin phosphorylation by Rho-associated kinase and myosin phosphatase. *J. Cell Biol.* 141:409–418.
Gallo, G., and P.C. Letourneau. 2000. Neurotrophins and the dynamic regulation of the neuronal cytoskeleton. *J. Neurobiol.* 44:159–173.
Goldberg, D.J., and D.Y. Wu. 1995. Inhibition of formation of filopodia after axotomy by inhibitors of protein tyrosine kinases. *J. Neurobiol.* 27:553–560.
Goldberg, J.I., and S.B. Kater. 1989. Expression and function of the neurotransmitter serotonin during development of the *Helisoma* nervous system. *Dev. Biol.* 131:483–495.
Haydon, P.G., D.P. McCobb, and S.B. Kater. 1984. Serotonin selectively inhibits growth cone motility and synaptogenesis of specific identified neurons. *Science*. 226:561–564.
Igarashi, M., W.W. Li, Y. Sudo, and M.C. Fishman. 1995. Ligand-induced growth cone collapse: amplification and blockade by variant GAP-43 peptides. *J. Neurosci.* 15:5660–5667.
Izzard, C.S., and L.R. Lochner. 1980. Formation of cell-to-substrate contacts during fibroblast motility: an interference-reflection study. *J. Cell Sci.* 42:81–116.
Jalink, K., E.J. van Corven, and W.H. Moolenaar. 1990. Lysophosphatidic acid, but not phosphatidic acid, is a potent Ca2(+)-mobilizing stimulus for fibroblasts. Evidence for an extracellular site of action. *J. Biol. Chem.* 265:12232–12239.
Jian, X., H. Hidaka, and J.T. Schmidt. 1994. Kinase requirement for retinal growth cone motility. *J. Neurobiol.* 25:1310–1328.
Jin, Z., and S.M. Strittmatter. 1997. Rac1 mediates collapsin-1-induced growth cone collapse. *J. Neurosci.* 17:6256–6263.
Kater, S.B., and L.R. Mills. 1991. Regulation of growth cone behavior by calcium. *J. Neurosci.* 11:891–899.
Kimura, K., M. Ito, M. Amano, K. Chihara, Y. Fukata, M. Nakafuku, B. Yamamori, J. Feng, T. Nakano, K. Okawa, et al. 1996. Regulation of myosin phosphatase by Rho and Rho-associated kinase (Rho-kinase). *Science*. 273: 245–248.
Kozma, R., S. Sarner, S. Ahmed, and L. Lim. 1997. Rho family GTPases and neuronal growth cone remodelling: relationship between increased complexity induced by Cdc42Hs, Rac1, and acetylcholine and collapse induced by RhoA and lysophosphatidic acid. *Mol. Cell. Biol.* 17:1201–1211.
Kuhn, T.B., M.D. Brown, C.L. Wilcox, J.A. Raper, and J.R. Bamburg. 1999. Myelin and collapsin-1 induce motor neuron growth cone collapse through different pathways: inhibition of collapse by opposing mutants of rac1. *J. Neurosci.* 19:1965–1975.
Lanier, L.M., and F.B. Gertler. 2000. From Abl to actin: Abl tyrosine kinase and associated proteins in growth cone motility. *Curr. Opin. Neurobiol.* 10: 80–87.
Lanier, L.M., M.A. Gates, W. Witke, A.S. Menzies, A.M. Wehman, J.D. Macklis, D. Kwiatkowski, P. Soriano, and F.B. Gertler. 1999. Mena is required for neurulation and commissure formation. *Neuron*. 22:313–325.
Lankford, K.L., F.G. DeMello, and W.L. Klein. 1988. D1-type dopamine receptors inhibit growth cone motility in cultured retina neurons: evidence that neurotransmitters act as morphogenic growth regulators in the developing central nervous system. *Proc. Natl. Acad. Sci. USA*. 85:4567–4571.
Letourneau, P.C. 1979. Cell-substratum adhesion of neurite growth cones, and its role in neurite elongation. *Exp. Cell Res.* 124:127–138.
Lin, C.H., and P. Forscher. 1993. Cytoskeletal remodeling during growth cone–target interactions. *J. Cell Biol.* 121:1369–1383.
Lin, C.H., E.M. Espreafico, M.S. Mooseker, and P. Forscher. 1996. Myosin drives retrograde F-actin flow in neuronal growth cones. *Neuron*. 16:769–782.
Luo, Y., D. Raible, and J.A. Raper. 1993. Collapsin: a protein in brain that induces the collapse and paralysis of neuronal growth cones. *Cell*. 75:217–227.
Luo, Y., I. Shepherd, J. Li, M.J. Renzi, S. Chang, and J.A. Raper. 1995. A family of molecules related to collapsin in the embryonic chick nervous system. *Neuron.* 14:1131–1140.
Mackay, D.J., F. Esch, H. Furthmayr, and A. Hall. 1997. Rho- and rac-dependent assembly of focal adhesion complexes and actin filaments in permeabilized fibroblasts: an essential role for ezrin/radixin/moesin proteins. *J. Cell Biol.* 138:927–938.
Mallavarapu, A., and T. Mitchison. 1999. Regulated actin cytoskeleton assembly at filopodium tips controls their extension and retraction. *J. Cell Biol.* 146:1097–1106.
Mangeat, P., C. Roy, and M. Martin. 1999. ERM proteins in cell adhesion and membrane dynamics. *Trends Cell Biol.* 9:187–192.
McCobb, D.P., P.G. Haydon, and S.B. Kater. 1988. Dopamine and serotonin inhibition of neurite elongation of different identified neurons. *J. Neurosci. Res.* 19:19–26.
Meima, L., I.J. Kljavin, P. Moran, A. Shih, J.W. Winslow, and I.W. Caras. 1997. AL-1-induced growth cone collapse of rat cortical neurons is correlated with REK7 expression and rearrangement of the actin cytoskeleton. *Eur. J. Neurosci.* 9:177–188.
Moolenaar, W.H., O. Kranenburg, F.R. Postma, and G.C. Zondag. 1997. Lysophosphatidic acid: G-protein signalling and cellular responses. *Curr. Opin. Cell Biol.* 9:168–173.
Mueller, B.K. 1999. Growth cone guidance: first steps towards a deeper understanding. *Annu. Rev. Neurosci.* 22:351–388.
Muir, D., K. Sonnenfeld, and S. Berl. 1989. Growth cone advance mediated by fibronectin-associated filopodia is inhibited by a phorbol ester tumor promoter. *Exp. Cell Res.* 180:134–149.
Noegel, A., W. Witke, and M. Schleicher. 1987. Calcium-sensitive non-muscle alpha-actinin contains EF-hand structures and highly conserved regions. *FEBS Lett.* 221:391–396.
O'Connor, T.P., and D. Bentley. 1993. Accumulation of actin in subsets of pioneer growth cone filopodia in response to neural and epithelial guidance cues in situ. *J. Cell Biol.* 123:935–948.
Paglini, G., P. Kunda, S. Quiroga, K. Kosik, and A. Caceres. 1998. Suppression of radixin and moesin alters growth cone morphology, motility, and process formation in primary cultured neurons. *J. Cell Biol.* 143:443–455.
Polak, K.A., A.M. Edelman, J.W. Wasley, and C.S. Cohan. 1991. A novel calmodulin antagonist, CGS 9343B, modulates calcium-dependent changes in neurite outgrowth and growth cone movements. *J. Neurosci.* 11:534–542.
Rochlin, M.W., K. Itoh, R.S. Adelstein, and P.C. Bridgman. 1995. Localization of myosin II A and B isoforms in cultured neurons. *J. Cell Sci.* 108:3661–3670.
Ruchhoeft, M.L., and W.A. Harris. 1997. Myosin functions in *Xenopus* retinal ganglion cell growth cone motility in vivo. *J. Neurobiol.* 32:567–578.
Sebok, A., N. Nusser, B. Debreceni, Z. Guo, M.F. Santos, J. Szeberenyi, and G. Tigyi. 1999. Different roles for RhoA during neurite initiation, elongation, and regeneration in PC12 cells. *J. Neurochem.* 73:949–960.
Spencer, G.E., K. Lukowiak, and N.I. Syed. 2000. Transmitter-receptor interactions between growth cones of identified lymnaea neurons determine target cell selection in vitro. *J. Neurosci.* 20:8077–8086.
Tessier-Lavigne, M. 1994. Axon guidance by diffusible repellants and attractants. *Curr. Opin. Genet. Dev.* 4:596–601.
Tessier-Lavigne, M., and C.S. Goodman. 1996. The molecular biology of axon guidance. *Science*. 274:1123–1133.
Verkhovsky, A.B., T.M. Svitkina, and G.G. Borisy. 1995. Myosin II filament assemblies in the active lamella of fibroblasts: their morphogenesis and role in the formation of actin filament bundles. *J. Cell Biol.* 131:989–1002.
Welnhofer, E.A., L. Zhao, and C.S. Cohan. 1997. Actin dynamics and organization during growth cone morphogenesis in *Helisoma* neurons. *Cell Motil. Cytoskeleton*. 37:54–71.
Welnhofer, E.A., L. Zhao, and C.S. Cohan. 1999. Calcium influx alters actin bundle dynamics and retrograde flow in *Helisoma* growth cones. *J. Neurosci.* 19:7971–7982.
Williams, D.K., and C.S. Cohan. 1994. The role of conditioning factors in the formation of growth cones and neurites from the axon stump after axotomy. *Brain Res. Dev. Brain Res.* 81:89–104.
Wong, R.G., R.D. Hadley, S.B. Kater, and G.C. Hauser. 1981. Neurite outgrowth in molluscan organ and cell cultures: the role of conditioning factors. *J. Neurosci.* 1:1008–1021.
Wylie, S.R., P.J. Wu, H. Patel, and P.D. Chantler. 1998. A conventional myosin motor drives neurite outgrowth. *Proc. Natl. Acad. Sci. USA*. 95:12967–12972.
Yamakita, Y., S. Ono, F. Matsumura, and S. Yamashiro. 1996. Phosphorylation of human fascin inhibits its actin binding and bundling activities. *J. Biol. Chem.* 271:12632–12638.
Zheng, J.Q., M. Felder, J.A. Connor, and M.M. Poo. 1994. Turning of nerve growth cones induced by neurotransmitters. *Nature*. 368:140–144.
Zheng, J.Q., J.J. Wan, and M.M. Poo. 1996. Essential role of filopodia in chemotropic turning of nerve growth cone induced by a glutamate gradient. *J. Neurosci.* 16:1140–1149.
Zigmond, S.H., R. Furukawa, and M. Fechheimer. 1992. Inhibition of actin filament depolymerization by the *Dictyostelium* 30,000-D actin-bundling protein. *J. Cell Biol.* 119:559–567.